Journal of Power Sources 609 (2024) 234710

Contents lists available at ScienceDirect

Journal of Power Sources

journal homepage: www.elsevier.com/locate/jpowsour

Covalent surface grafting of $Ti_3C_2T_x$ flakes for enhancement of symmetric supercapacitor performance

Vasilii Burtsev [a], Elena Miliutina [a], Vera Shilenko [a], Karolina Kukrálová [a], Andrei Chumakov [b], Matthias Schwartzkopf [b], Václav Švorčík [a], Jan Lancok [c], Sergii Chertopalov [c], Oleksiy Lyutakov [a,*]

[a] Department of Solid State Engineering, University of Chemistry and Technology, 16628, Prague, Czech Republic
[b] Deutsches Elektronen-Synchrotron DESY, Notkestr. 85, 22607, Hamburg, Germany
[c] Institute of Physics of the Czech Academy of Sciences, Na Slovance 1999/2, 18200, Prague, Czech Republic

HIGHLIGHTS

- The covalent surface modification of $Ti_3C_2T_x$ flakes was proposed.
- Applied procedure allows to enhance the functionality of MXene-based supercapacitors.
- The increase of supercapacitance different conditions was observed.
- The surface grafting prevents the supercapacitor degradation.
- Flakes grafting decelerates the spontaneous discharge rate in open circuit mode.

ARTICLE INFO

Keywords:
$Ti_3C_2T_x$
Surface termination
Covalent grafting
Plasmon assisted chemistry
Supercapacitor

ABSTRACT

In this work the covalent surface modification of MXene flakes ($Ti_3C_2T_x$) was proposed for the increasing of the performance of subsequently created symmetric supercapacitor. Covalent surface modification was performed with utilization of diazonium salts (hydrophobic or hydrophilic) and plasmon-assisted photochemistry. Applied procedure allows to block the reactive (weak and/or catalytically active) sites on flakes surface and increase the flakes interplanar spacing, both enhancing the functionality of an MXene-based supercapacitor. Especially pronounced positive effect gives the surface modification with hydrophilic chemical moieties. In particular, we observed increase of supercapacitance from 197 to 284 F g^{-1} in acidic and from 86 to 142 F g^{-1} in alkaline conditions for flakes grafted with $–C_6H_4–COOH$ chemical moieties at scan rate 20 mV/s. The flakes grafted with hydrophobic chemical moieties allow to achieve almost constant value of supercapacitance for different speed of charge discharge. In addition, the surface grafting prevents the supercapacitor degradation and decelerates the spontaneous discharge in open circuit mode. These results suggest strategy for further improvement of MXene-based supercapacitors as energy storage device.

1. Introduction

Flexible supercapacitors, based on 2D materials, have attracted considerable attention as a promising energy storage systems for portable and wearable electronic devices [1–3]. Among 2D materials the MXenes are considered as especially promissing materials for flexible supercapacitor due to their excellent electronic conductivity, reversible surface redox capability, and good hydrophilicity [4–7]. The general formula of MXenes is $M_{n+1}X_nT_x$, where M represents transition metal(s), X – carbon and/or nitrogen, and T_x – surface termination groups [8]. The interaction of MXenes with surrounding electrolyte and related supercapacitor performance strongly depend on surface terminations (T_x) [9]. In a common way the MXenes are prepared by etching of corresponding MAX phase with utilization of "small" H^+ cations and F^- counter-ions [10]. However, this route leads to the formation of –F surface termination and presence of this chemical group significantly restricts ions

* Corresponding author.
E-mail address: lyutakoo@vscht.cz (O. Lyutakov).

https://doi.org/10.1016/j.jpowsour.2024.234710
Received 25 January 2024; Received in revised form 23 April 2024; Accepted 10 May 2024
Available online 14 May 2024

mobility in MXene films and ruins functionality of MXenes as an active supercapacitor material [11–13]. In addition, the MXene flakes tend to agglomeration and restacking during film formation, which also complicate the ion diffusion in the MXene thin films and in turn eliminate advantages of MXene based supercapacitors [14,15]. In particular, flakes restacking can lead to some increase in thin film conductivity, but significantly restrict supercapacitance performance [16].

To decrease the negative impact of fluor termination and flakes restacking various strategies have been proposed. In a common way, intercalation of the flakes with metal ions before supercapacitor utilization was used to prevent restacking [17,18]. Alternatively, a combination of MXenes with other materials that serve as electrochemically active or passive spacers has been proposed for the same objective [19–24]. Alternatively, flakes preparation using alternative etching/delamination route, with the aim to dominantly create the = O, –OH, –Cl, $–NH_2$ or = S surface termination, instead of –F has also been successfully demonstrated for significant increase of supercapacitance of MXene based thin films [25–29]. Finally, the undesired –F terminations can be removed by various post-preparative treatments, including thermal annealing, hydro/solvothermal processing or flakes interaction with molten inorganic salts [30–33]. However, surface exchange reactions occur at high temperatures 300–600 °C under "strong" chemical environment and such conditions can damage flakes 2D structure or introduce defects, which serve as a subsequent degradation centres [9, 32].

In our previous work we demonstrated the simple photochemical route for tuning of MXene surface termination using diazonium salts and plasmon-assisted chemistry [34,35]. Our approach is based on plasmon excitation on MXene flakes surface, subsequent plasmon-induced decomposition of diazonium salt(s), creation of highly reactive radicals and their subsequent grafting to flakes. In this work, we investigate the impact of organic moieties grafting on the functionality of MXenes-based supercapacitors and demonstrate the attractiveness of such approach on the way to supercapacitors improvement [36].

2. Results and discussion

General concept of created MXene surface grafting with organic chemical moieties is presented in Fig. 1. First, the $Ti_3C_2T_x$ flakes, prepared by LiF/HCl etching and ultrasound delamination were dispersed in water/methanol solution. The 4-carboxybenzenediazonium tosylate and 3,5-Bis(trifluoromethyl) benzenediazonium tosylate salts were added to $Ti_3C_2T_x$ suspension and reaction mixture was illuminated during 2 h at 780 nm wavelength, corresponding to flakes plasmon absorption band (Fig. S1). Under these conditions, diazonium salts undergo degradation, with the cleavage of the nitrogen molecule and the creation of highly reactive organic radicals, which attack the surface of the flakes. As a result, organic moieties are covalently grafted to $Ti_3C_2T_x$, with the formation of Ti–C_6H_4–R bonds or through oxygen bridges and the attachment of chemical moieties (Fig. 1C) [36]. As a results of plasmon-assisted chemistry, the tuning of flakes grafting occurs with the creation of Ti–*R* or Ti–*O*-*R* (where R = –C_6H_4–COOH or –C_6H_4-CF_3) chemical bonds. Modified MXene flakes were subsequently designated as Ti_3C_2–COOH *or* Ti_3C_2-CF_3, depending on the used diazonium salt and grafted organic moieties. Subsequently, thin MXene films were created using vacuum-assisted filtration and arranged in a symmetric supercapacitor with utilization of 25 μm thick Celgard 3401 membrane.

The conformation of $Ti_3C_2T_x$ flakes grafting is presented in Fig. 2. First Raman spectroscopy indicates the appearance of several additional vibration bands (Fig. 2A), which can be attributed to the chemical structure of grafted organic moieties (detailed peaks affiliation is given in Table S1). Similar results were also observed with the use of Fourier-transform infrared spectroscopy (FTIR) measurements, which also confirmed the presence of a benzene ring and –COOH or –CF3 chemical moieties (Fig. S2). The modification of flakes surface termination was also accompanied by the apparent changes in $Ti_3C_2T_x$ thin films surface wettability – from initial 67° up to 28° in the case of –C_6H_4–COOH moieties. However, after flakes grafting with hydrophobic –C_6H_4-CF_3 chemical moieties the wettability increases up to 92° (Fig. 2B). The surface grafting with additional moieties was also confirmed by XPS (Fig. 2C and D). The increase of surface carbon concentration, as well as screening of characteristic Ti signal after the flakes grafting, is well evident on survey XPS spectra (or from calculated surface elemental composition). In particular, the grafting with –C_6H_4–COOH results in an oxygen surface concentration increase, while the grafting with C_6H_4-CF_3 leads to a –F concentration increase. Important absence of the characteristic nitrogen signal confirms the release of N_2 molecules and formation of "true" covalent bond between flakes and created organic radicals (Fig. S3). The morphology of $Ti_3C_2T_x$ flakes was confirmed using atomic force microscopy (AFM) measurements, which revealed the 2D nature of the materials (lateral size was varied in the 300–1000 nm range and did not change after grafting – Fig. S4).

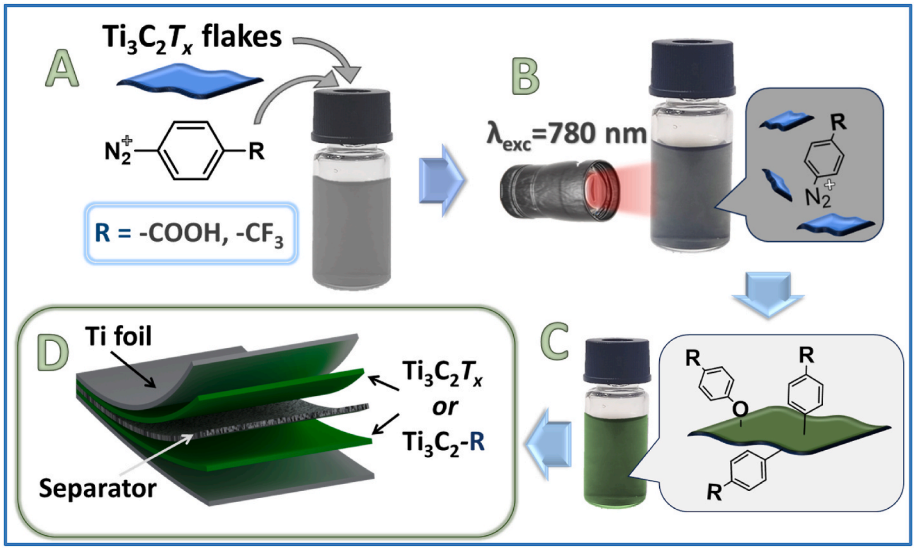

Fig. 1. Schematic representation of $Ti_3C_2T_x$ flakes modification – mixing of flakes suspension with diazonium salt (A) and subsequent illumination of created suspension (B) results in the creation of organic radicals which are grafted to flakes surface through -*O*- bridge or directly to Ti atoms by substitution mechanism (C). In the next step, the pristine or grafted MXene films are arranged in a symmetric supercapacitor design (D).

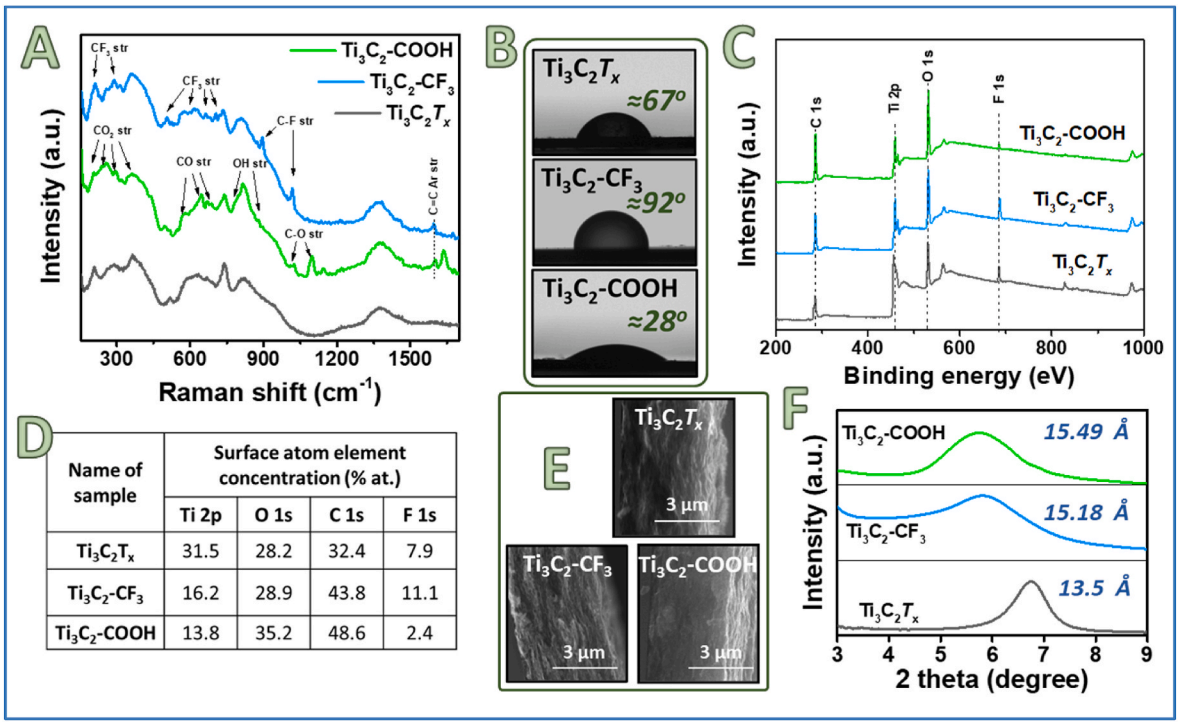

Fig. 2. Confirmation of $Ti_3C_2T_x$ flakes grafting: (A) – Raman spectra of pristine and grafted flakes; (B) – water contact angle as a function of pristine or tuned surface termination of $Ti_3C_2T_x$; (C, D) – XPS survey spectra and calculated surface elemental composition for pristine and grafted flakes; (E) – cross-section image of $Ti_3C_2T_x$ films; (F) – grafting induced shift of low angle XRD peak (and corresponding values of interplanar distance) observed after arrangement of flakes in thin films.

The cross-sectional SEM images of the thin films created from pristine or grafted flakes indicate a closely-packed arrangement of flakes (for both pristine and grafted flakes – Fig. 2E). The thickness of created films, estimated from SEM was in 4–5 μm range. In turn, the low-angle part of XRD patterns (Fig. 2D) indicates the apparent shift of low-angle (002) peak in the case of grafted flakes, indicating an increase in the interlayer spacing, due to the steric reasons (full XRD patterns are presented in Fig. S5). In particular, the calculated values of interplanar spacing are 13.5 Å for pristine $Ti_3C_2T_x$ flakes, 15.5 Å and 15.2 Å for grafted Ti_3C_2–COOH and Ti_3C_2-CF_3 flakes. It can be preliminarily supposed that such increase of interplanar spacing can ensure additional channels for ion(s) transfer and, in this way, increase the supercapacitance of MXene films.

In the next step, the MXene films were arranged in a symmetric supercapacitor scheme with activated Celgard 3401 membrane. To demonstrate supercapacitor functionality, different electrochemical and stability tests were performed in acidic and alkaline conditions. The potential range, corresponding to true supercapacitor behaviour was determined as a function of surface functionality: Fig. 3A–C show results obtained in acidic (1 M H_2SO_4) conditions. The pristine MXene has almost rectangular cyclic voltammetry (CVA) shapes in 0–0.6 V potential range. The subsequent increase in potential range leads to gradual deviation from rectangular shape, indicating the beginning of an undesired redox process. The grafting with –C_6H_4–COOH results in available potential range expanded up to 0–0.8 V and makes the CVA curves even more “ideal”, i.e. closer to a perfect rectangle. Such results could be expected, since grafting of organic chemical moieties commonly proceeds on surface defects (or –OH surface termination) and these places are prone to oxidation which in turn support the redox process (undesired water splitting) [37,38]. So that, blocking of these places with organic moieties may increase the flakes stability, decrease the undesired (in the present case) flakes catalytic activity and expand in this way the available potential range [39,40]. Some increase (but just to 0–0.65 V) of available potential range was also observed in the case of flakes surface termination with hydrophobic –C_6H_4-CF_3 chemical moieties. However, in this case the apparent deviation from rectangular shape is observed at relatively low potential, above 0.7 V. Such undesired deviation can be rather attributed to ions diffusion controlled processes, which are restricted by hydrophobic surface termination.

After determination of more suitable potential range, series of CVA measurements were performed at different scan rates for symmetric supercapacitors, constructed from pristine and grafted flakes. In all cases, the potential ranges corresponding to true supercapacitor behaviours were used and obtained results are presented in Fig. 3D–F. As could be expected the area of CVA curves increases with increasing scan rate [41,42]. The supercapacitance value, calculated from the CVA curves are shown in Fig. 3G as a function of the scan rate. As is evident the flakes grafting with hydrophilic –COOH chemical moieties results in supercapacitance increase by ca 40 % for all scan rates. The surface modification with hydrophobic –CF_3 chemical moieties oppositely reduces the supercapacitance. For both $Ti_3C_2T_x$ and Ti_3C_2–COOH flakes an obvious decrease of supercapacitance is observed with increasing scan rate. This trend is less pronounced in the case of –COOH grafted flakes, which effect can be considered as an additional benefit provided by surface chemistry modification. Finally, in the case of Ti_3C_2-CF_3 flakes the supercapacitance was found to be almost independent on the scan rate. So, MXene flakes surface modification with hydrophilic chemical moieties results in obvious increase in supercapacitance. The grafting with hydrophobic chemical moieties leads to a supercapacitance decrease but makes it less sensitive toward device charge/discharge rate.

The results of CVA scans obtained in 1 M KOH solution are presented in Fig. 4. Like in the previous case, the potential range of true supercapacitor behaviour was determined first (Fig. 4A–C). We observe nearly rectangular behaviour for pristine $Ti_3C_2T_x$ supercapacitor in 0–0.8 V range. By grafting this potential range is expanded up to 0–1.0 V in the case of Ti_3C_2–COOH flakes and up to 0–1.1 V in the case of Ti_3C_2-CF_3 flakes. So, grafting with chemical moieties increase the working range of the supercapacitor even in the case of alkaline electrolyte. The CVA scans performed at different rates are presented in Fig. 4 D-F. Excellent

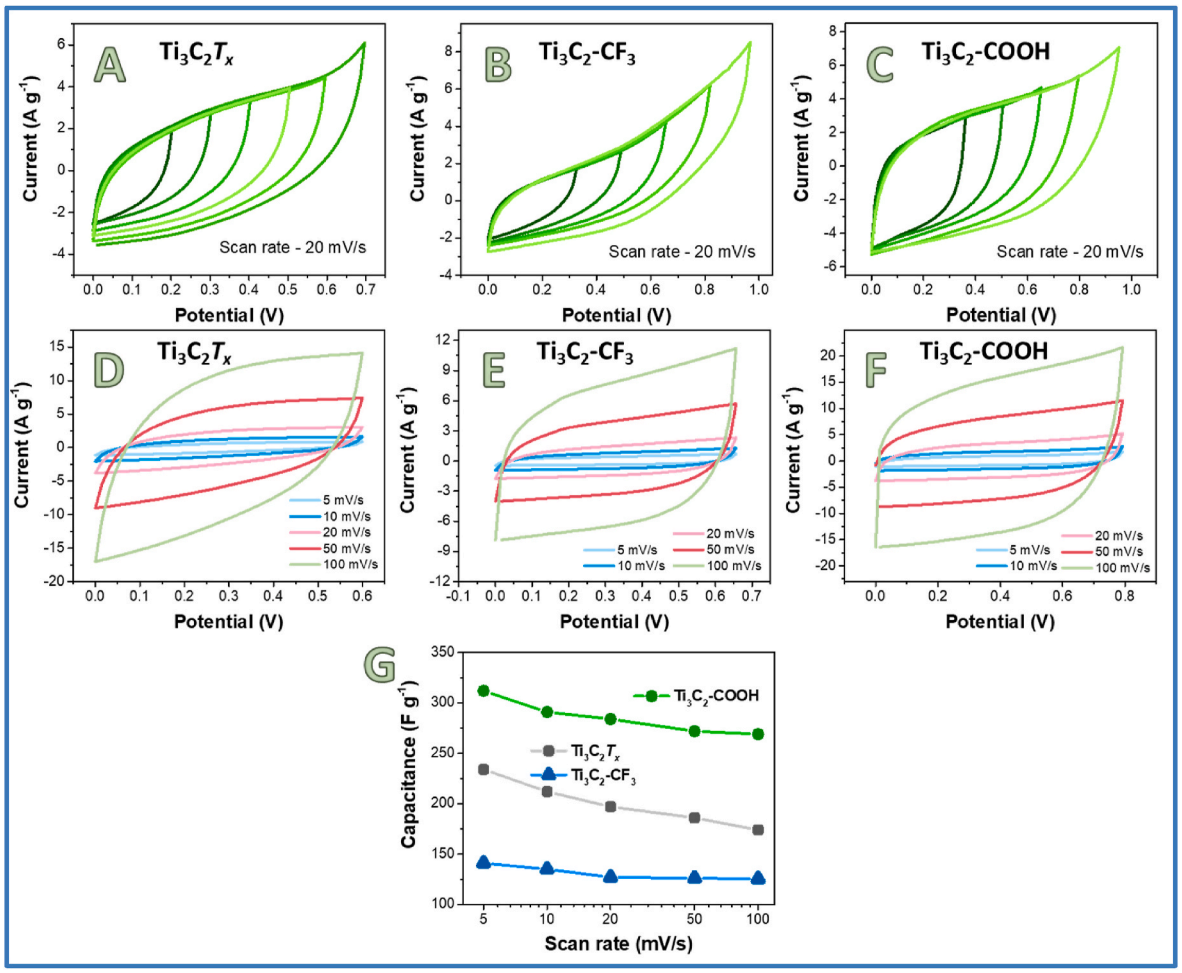

Fig. 3. (A–C) – determination of available potential range for true supercapacitor behavior (in 1 M H_2SO_4 solution) of symmetric device, created from $Ti_3C_2T_x$ films (pristine or grafted) separated by Celgard 3401 membrane; (D–F) – CVA scans, performed at the different scan rate for symmetric supercapacitors created from pristine or grafted flakes; (G) – calculated values of supercapacitance as a function of scan rate.

results are observed for Ti_3C_2–COOH flakes (Fig. 4E), with almost ideal CVA shape. The calculated value of supercapacitance was found to be larger by about 70 % than that in the case of pristine flakes. Oppositely, flakes modification with hydrophobic chemical moieties significantly decreases the device supercapacitance. Finally, supercapacitance dependence on the scan rate is presented in Fig. 4G. The apparent decrease of supercapacitance with an increase of charge/discharge rate was observed for pristine $Ti_3C_2T_x$ and Ti_3C_2–COOH flakes. In the case of hydrophilic modification, however, the supercapacitance was found to be almost constant, like in the previous case with acidic electrolyte. We also estimated the supercapacitor(s) performance of the created device in the neutral electrolyte (Fig. S6). In this case, a similar trend was observed: the highest supercapacitance value (130 $A*g^{-1}$) was observed for flakes terminating with –COOH chemical moieties. In turn, grafting with hydrophilic chemical moieties results in an apparent decrease of supercapacitance, but makes it less sensitive towards the changing of charging/discharging rate.

Results of CVA measurement were additionally checked by charge-discharge measurements, also performed in alkaline and acidic medium using symmetric supercapacitor constructed from pristine and grafted flakes (Fig. S7 and Fig. 5 A, B). The close to linear curves also indicate the true supercapacitor behaviour, without the presence of redox process. Moreover, calculated values of supercapacitance also correlate well with CVA results – the highest capacitance is observed for –C_6H_4–COOH flakes (264 F g^{-1} in acidic and 133 F g^{-1} in alkaline electrolytes), the moderate capacitance is observed in the case of pristine flakes (187 F g^{-1} in acidic and 73 F g^{-1} in alkaline electrolytes) and the lower capacitance is found for flakes grafted with –C_6H_4-CF_3 chemical moieties (131 F g^{-1} in acidic and 14 F g^{-1} in alkaline electrolytes). We also estimated the stability of the created symmetric supercapacitors as a function of flakes modification. The normed supercapacitance retention is presented in Fig. 5A and B after up to 10 000 cycles of charge/discharge in both, acidic and alkaline electrolytes. As is evident, the supercapacitance of pristine flakes gradually decreases with increasing cycles, indicating gradual degradation of flakes and corresponding worsening of supercapacitor functionality. This phenomenon is accompanied by the appearance of characteristic TiO_2 Raman bands, especially pronounced in the case of acidic electrolyte (Fig. 5C). In the case of previously grafted flakes, the appearance of characteristic TiO_2 bands was significantly suppressed, while the stability of the device based on grafted flakes was found to be significantly better. In this case, the increase in overall stability should be attributed to previous flakes grafting, which is performed at the “weaker” surface sites. It is well known that $Ti_3C_2T_x$ undergoes oxidation, which starts at the edges or –OH terminated groups and leads to the formation of titanium oxide with a corresponding loss of the conductivity of the flakes (which, in a decrease, in turn, results in the decrease of the supercapacitor). The grafting proposed here results in the attachment of chemical moieties to the edges of the flakes and –OH terminated surface groups, thereby preventing the initial stages of oxidation. As a result, the functionality of thin films created from grafted flakes is increased. Additional SEM measurements, performed after stability tests, also

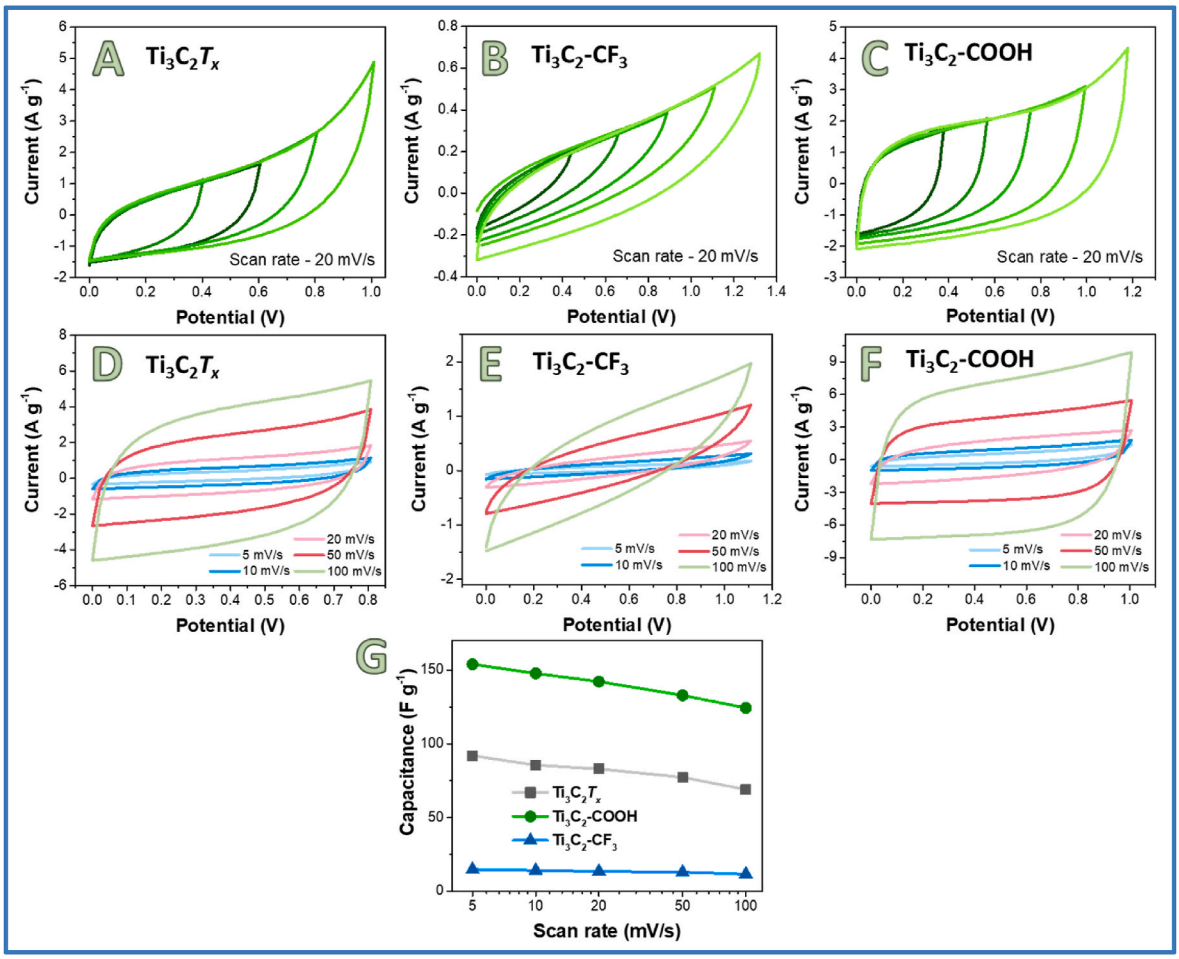

Fig. 4. (A–C) – determination of available potential range for true supercapacitor behavior (in 1 M KOH solution) of symmetric device, created from $Ti_3C_2T_x$ films (pristine or grafted) separated by Celgard 3401 membrane; (D–F) – CVA scans, performed at the different scan rate for symmetric supercapacitors created from pristine or grafted flakes; (G) – calculated values of supercapacitance as a function of scan rate.

indicate the conservation of the structure and morphology of the Ti_3C_2-CF_3 and Ti_3C_2–COOH thin films (Fig. S8).

Another parameter, which should be considered in the case of MXene based supercapacitors is their gradual discharge in open circuit, which can occur due to parasitic reaction and is especially pronounced in the acidic or alkaline electrolytes, as has been demonstrated recently [43]. In our case we also observe the rapid discharge, especially pronounced in the case of pristine flakes. However, the grafting of flakes with both, $–C_6H_4–$COOH and $–C_6H_4$-CF_3 chemical moieties prolongate the spontaneous discharge times significantly and makes the device more practically applicable (Fig. 5 E, F). Both, increase of supercapacitor stability and deceleration of spontaneous device discharge should be attributed to the changes in flakes surface termination. In particular, the grafting commonly proceeds on flakes defects, edges or –OH chemical group (in the last case with the formation of oxygen bridges). Flakes oxidation commonly starts at these surface sites and their blocking significantly prolongate the flakes lifetime and conserve the supercapacitance value (at least in the potential range, corresponding to top true capacitance). Moreover, the same sites are known to be a catalytically active and supporting the parasitic reaction, leading in turn to spontaneous supercapacitor discharge in open circuit. Like in the previous case, the blocking of these surface sites can prevent the reaction occurrence and conserve the charge collected in MXene film(s) for longer time [39,40].

We also demonstrated the changes in surface distance induced by surface grafting using the GIWAXS measurements with to the humidity cell [34,44]. Fig. 5D shows the apparent shift of flakes interplanar distance after the immersion of MXene thin films in water. Thus, parameter was shifted from 0.494 $Å^{-1}$ to 0.446 $Å^{-1}$ for pristine flakes, from 0.438 $Å^{-1}$ to 0.383 $Å^{-1}$ for flakes grafted with $–C_6H_4–$COOH, and from 0.46 $Å^{-1}$ to 0.43 $Å^{-1}$ for flakes grafted with $–C_6H_4$-CF_3 chemical moieties. So, the higher amount of water molecules penetrates in the flakes, in the case of $–C_6H_4–$COOH grafting, while flakes surface decoration partially prevents the water molecules penetration (also supported by QCM measurements – Fig. S9).

Finally, we also estimated our results with previously published ones (Table 1). As is evident, the value of supercapacitance, reached in our case is similar to the commonly obtained with MXene-based materials (except pseudo-supercapacitors cases are reported through the combination of $Ti_3C_2T_x$ flakes with redox-active materials). On the other hand, proposed here, utilization of surface chemistry tuning allows one to increase the lifetime of the supercapacitor, partially prevent the spontaneous device discharging, as well as increase the working potential (this important parameter is often not considered in publications).

3. Conclusion

In this paper the impact of covalent surface modification of $Ti_3C_2T_x$ flakes on the functionality of subsequently created symmetric supercapacitor was investigated. The flakes surface was grafted with hydrophilic and hydrophobic chemical moieties through the plasmon-assisted diazonium chemistry. The surface modification was confirmed using the XPS and Raman spectroscopy. After confirmation of tuning via surface chemistry, the properties and functionality of created supercapacitor(s) were investigated in both alkaline and acidic media. It was found that

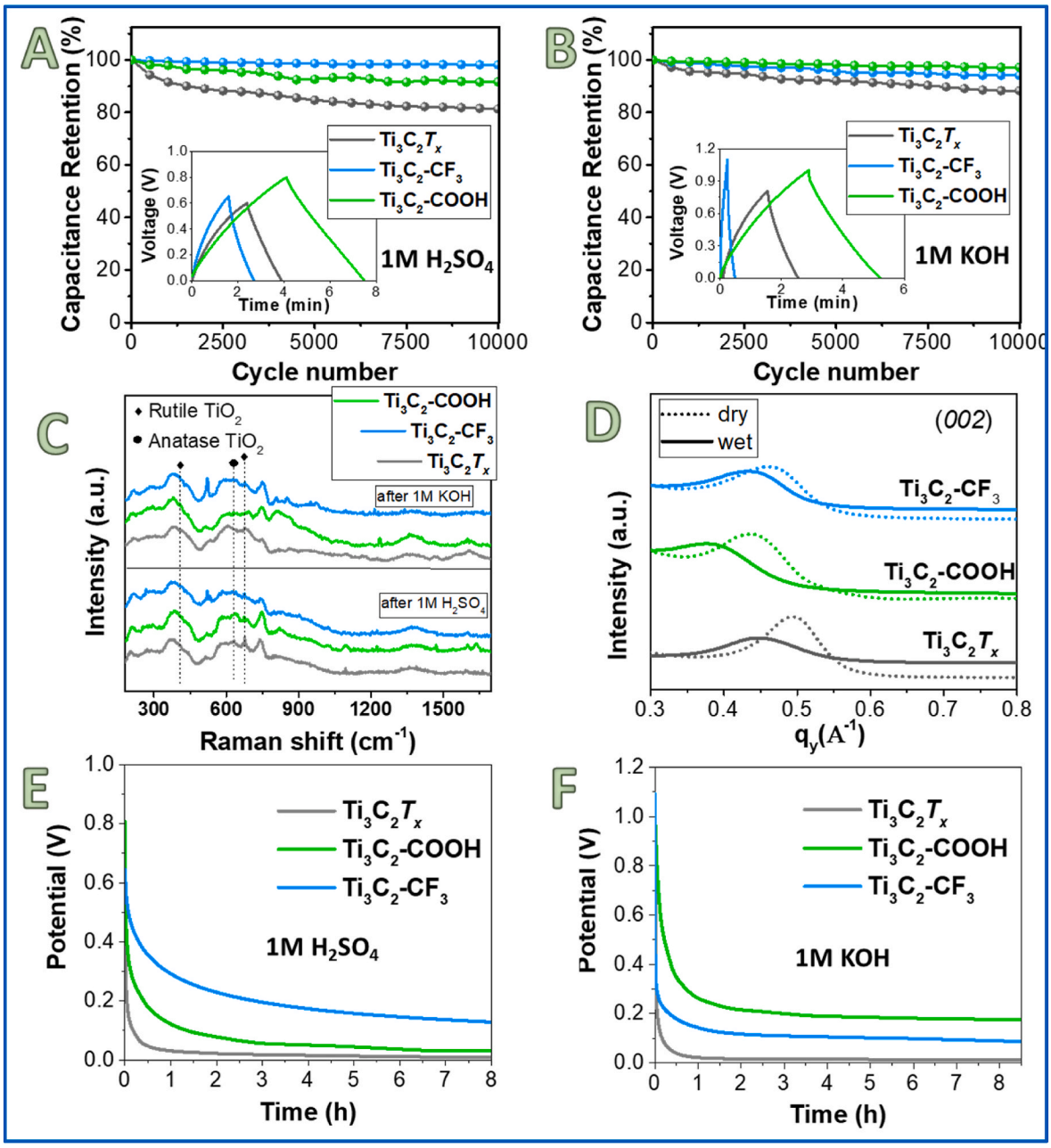

Fig. 5. (A, B) – supercapacitance retention during subsequent cycles of charge/discharge measured for pristine and grafted flakes, inserts show the typical cycle of charge/discharge, (C) – Raman spectra of pristine and grafted flakes, measured after 10 000 charge/discharge cycles for corresponding supercapacitor in acidic electrolyte; (D) – GIWAXS measurements results, revealing the shift of low angle peak position due to water molecules penetration between flakes; (E, F) – supercapacitor discharge measured in open circuit mode in acidic or alkaline conditions.

the covalent surface modification expands the supercapacitor operation range (in true supercapacitor behaviour terms). The supercapacitance is increased by the grafting with hydrophilic chemical moieties. Oppositely, the grafting with hydrophobic groups results in supercapacitance decrease but makes the supercapacitance almost independent on charge/discharge rate. Moreover, surface grafting significantly increases the flakes stability during the charging/discharging cycling and partially prevent the supercapacitor spontaneous discharge in open-circuit regime. All observed phenomena and advantages of covalent modification of $Ti_3C_2T_x$ can be attributed to increased distance between flakes (with creation of additional ion channels) as well as to blocking of "undesired" catalytically-active and/or unstable surface sites.

4. Experimental section

Detailed information regarding the experimental techniques, $Ti_3C_2T_x$ synthesis and modification, supercapacitor fabrication and characterization, as well as capacitance calculations, can be found in the Supplementary Information.

CRediT authorship contribution statement

Vasilii Burtsev: Validation, Methodology, Investigation. **Elena Miliutina:** Writing – review & editing, Methodology, Investigation. **Vera Shilenko:** Investigation. **Karolina Kukrálová:** Investigation. **Andrei Chumakov:** Investigation. **Matthias Schwartzkopf:** Investigation. **Václav Švorčík:** Writing – review & editing, Methodology, Formal

Table 1
Comparison of results obtained with previously published.

Material	Capacitance	Voltage window (V)	Electrolyte	References
MXene/AAC//AAC	177 F g^{-1}	2	7 M KOH	[45]
$Ti_3C_2T_x$-P	476.9 F g^{-1}	0.7	PVA–H_2SO_4 gel	[46]
d-$Ti_3C_2T_x$	323.7 F g^{-1}	0.8	3 M H_2SO_4	[47]
P-MXene/CPAQ-A	532.9 F g^{-1}	0.9	3 M H_2SO_4	[48]
MXene/CNFs	90 F g^{-1}	0.7	1 M H_2SO_4	[49]
MXene/Co_3O_4	374 F g^{-1}	0.6	6 M KOH	[50]
MXene/Co_3S_4	602 F g^{-1}	0.6	3 M KOH	[51]
$Ti_3C_2T_x$/PANI	272.5 F g^{-1}	0.8	PVA/H_2SO_4	[52]
MXene/α-Fe_2O_3@C	41 F g^{-1}	0.55	3 M NaOH	[53]
MXene/HGO	438 F g^{-1}	1	3 M H_2SO_4	[54]
MXene/MnO_2	612 F g^{-1}	0.85	0.2 M KOH	[55]
MXene/MnO_2/CC	511 F g^{-1}	0.8	3 M KOH	[56]
MXene/Graphdiyne nanotube	337.4 F g^{-1}	1	PVA-H_2SO_4 gel	[57]
1T-MWS/$Ti_3C_2T_x$	284 F g−1	0.6	1 M Na_2SO_4	[58]
Se/$Ti_3C_2T_x$	96 F g^{-1}	1.5	1 M Na_2SO_4	[59]
$Ti_3C_2T_x$ 'paper'	245 F g^{-1}	0.55	1 M H_2SO_4	[60]
MXene/PANI	579 F g^{-1}	0.6	3 M H_2SO_4	[61]
MXene/PPy	416 F g^{-1}	0.55	1 M H_2SO_4	[62]
MXene/RBP	738 F g^{-1}	0.8	1 M H_2SO_4	[63]
rGO/MXene@Fe_2O_3	893 F g^{-1}	0.6	PVA-KOH gel	[64]
rGO/ MXene@NiCo–P	1405 F g^{-1}	0.6	PVA-KOH gel	[64]
MXene/WO_3	297 F g^{-1}	1	0.5 M H_2SO_4	[65]
MXene	62 F g^{-1}	0.6	1 M NaOH	[66]
MXene	70 F g^{-1}	0.6	1 M KOH	[66]
MXene	69 F g^{-1}	0.6	0.5 M LiOH	[66]
MXene	26 F g^{-1}	0.65	1 M $Al_2(SO_4)_3$	[66]
MXene	81 F g^{-1}	0.75	0.5 M K_2SO_4	[66]
MXene-CF_3	131 F g^{-1}	0.65	1 M H_2SO_4	This work
MXene-COOH	264 F g^{-1}	0.8	1 M H_2SO_4	This work
MXene-CF_3	14 F g^{-1}	1.1	1 M KOH	This work
MXene-COOH	133 F g^{-1}	1	1 M KOH	This work
MXene-CF_3	26 F g^{-1}	0.9	1 M Na_2SO_4	This work
MXene-COOH	128 F g^{-1}	1	1 M Na_2SO_4	This work

analysis. **Jan Lancok:** Writing – review & editing, Formal analysis. **Sergii Chertopalov:** Writing – review & editing, Methodology, Investigation, Data curation. **Oleksiy Lyutakov:** Writing – original draft, Supervision, Conceptualization.

Declaration of competing interest

The authors declare that they have no known competing financial interests or personal relationships that could have appeared to influence the work reported in this paper.

Data availability

Data will be made available on request.

Acknowledgement

This work was supported by the GACR under project 21-09277S and by Project OP JAK_MeBioSys, No CZ.02.01. 01/00/22_008/0004634, of the Ministry of Education, Youth and Sports, which is co-funded by the European Union.

We acknowledge DESY (Hamburg, Germany), a member of the Helmholtz Association HGF, for the provision of experimental facilities. Parts of this research were carried out at PETRA III and we would like to thank P03 beamline staff for the assistance. Beamtime was allocated for proposal No. I-20230229 EC.

Appendix A. Supplementary data

Supplementary data to this article can be found online at https://doi.org/10.1016/j.jpowsour.2024.234710.

References

[1] L. Yao, Q. Wu, P. Zhang, J. Zhang, D. Wang, Y. Li, X. Ren, H. Mi, L. Deng, Z. Zheng, Scalable 2D hierarchical porous carbon nanosheets for flexible supercapacitors with ultrahigh energy density, Adv. Mater. 30 (2018) 1706054.
[2] K.S. Kumar, N. Choudhary, Y. Jung, J. Thomas, Recent advances in two-dimensional nanomaterials for supercapacitor electrode applications, ACS Energy Lett. 3 (2018) 482–495.
[3] H. Jeon, J.-M. Jeong, H.G. Kang, H.-J. Kim, J. Park, D.H. Kim, Y.M. Jung, S. Y. Hwang, Y.-K. Han, B.G. Choi, Scalable water-based production of highly conductive 2D nanosheets with ultrahigh volumetric capacitance and rate capability, Adv. Energy Mater. 8 (2018) 1800227.
[4] M. Hu, H. Zhang, T. Hu, B. Fan, X. Wang, Z. Li, Emerging 2D MXenes for supercapacitors: status, challenges and prospects, Chem. Soc. Rev. 49 (2020) 6666–6693.
[5] S. Venkateshalu, A.N. Grace, MXenes—a new class of 2D layered materials: synthesis, properties, applications as supercapacitor electrode and beyond, Appl. Mater. Today 18 (2020) 100509.
[6] Q. Jiang, Y. Lei, H. Liang, K. Xi, C. Xia, H.N. Alshareef, Review of MXene electrochemical microsupercapacitors, Energy Storage Mater. 27 (2020) 78–95.
[7] X. Wang, T.S. Mathis, K. Li, Z. Lin, L. Vlcek, T. Torita, N.C. Osti, C. Hatter, P. Urbankowski, A. Sarycheva, M. Tyagi, E. Mamontov, P. Simon, Y. Gogotsi, Influences from solvents on charge storage in titanium carbide MXenes, Nat. Energy 4 (2019) 241–248.
[8] Y. Gogotsi, B. Anasori, The rise of MXenes, ACS Nano 13 (2019) 8491–8494.
[9] M. Shen, W. Jiang, K. Liang, S. Zhao, R. Tang, L. Zhang, J.-Q. Wang, One-pot green process to synthesize MXene with controllable surface terminations using molten salts, Angew. Chem. Int. Ed. 60 (2021) 27013–27018.
[10] M. Alhabeb, K. Maleski, B. Anasori, P. Lelyukh, L. Clark, S. Sin, Y. Gogotsi, Guidelines for synthesis and processing of two-dimensional titanium carbide (Ti3C2Tx MXene), Chem. Mater. 29 (2017) 7633–7644.
[11] L. Guo, W.-Y. Jiang, M. Shen, C. Xu, C.-X. Ding, S.-F. Zhao, T.-T. Yuan, C.-Y. Wang, X.-Q. Zhang, J.-Q. Wang, High capacitance of MXene (Ti3C2Tx) through intercalation and surface modification in molten salt, Electrochim. Acta 401 (2022) 139476.
[12] C. Wang, H. Shou, S. Chen, S. Wei, Y. Lin, P. Zhang, Z. Liu, K. Zhu, X. Guo, X. Wu, P.M. Ajayan, L. Song, HCl-based hydrothermal etching strategy toward fluoride-free MXenes, Adv. Mater. 33 (2021) 2101015.
[13] M.M. Hasan, M.M. Hossain, H.K. Chowdhury, Two-dimensional MXene-based flexible nanostructures for functional nanodevices: a review, J. Mater. Chem. A 9 (2021) 3231–3269.
[14] M. Guo, W.-C. Geng, C. Liu, J. Gu, Z. Zhang, Y. Tang, Ultrahigh areal capacitance of flexible MXene electrodes: electrostatic and steric effects of terminations, Chem. Mater. 32 (2020) 8257–8265, https://doi.org/10.1021/acs.chemmater.0c02026.
[15] J. Li, H. Wang, X. Xiao, Intercalation in two-dimensional transition metal carbides and nitrides (MXenes) toward electrochemical capacitor and beyond, Energy Environ. Mater. 3 (2020) 306–322.
[16] A. Mateen, Z. Ahmad, S. Ali, N.U. Hassan, F. Ahmed, R.A. Alshgari, M. Mushab, Sayed M. Eldin, M.Z. Ansari, M.S. Javed, K.Q. Peng, Silicon intercalation on MXene nanosheets towards new insights into a superior electrode material for high-performance Zn-ion supercapacitor, J. Energy Storage 71 (2023) 108151.
[17] Q. Zhu, J. Li, P. Simon, B. Xu, Two-dimensional MXenes for electrochemical capacitor applications: progress, challenges and perspectives, Energy Storage Mater. 35 (2021) 630–660.
[18] J. Li, X. Yuan, C. Lin, Y. Yang, L. Xu, X. Du, J. Xie, J. Lin, J.J.A.E.M. Sun, Achieving high pseudocapacitance of 2D titanium carbide (MXene) by cation intercalation and surface modification, Adv. Energy Mater. 7 (2017) 1602725.
[19] J. Xu, J. You, L. Wang, Z. Wang, H. Zhang, MXenes serving aqueous supercapacitors: preparation, energy storage mechanism and electrochemical performance enhancement, Sustain. Mater. Technol. 33 (2022) e00490.
[20] M.H.M. Facure, K. Matthews, R. Wang, R.W. Lord, D.S. Correa, Y. Gogotsi, Pillaring effect of nanodiamonds and expanded voltage window of Ti3C2Tx supercapacitors in AlCl3 electrolyte, Energy Storage Mater. 61 (2023) 102919.
[21] S. Xu, Z. Li, G. Wei, Y. Wang, Y. Yang, Intercalation and surface modification of two-dimensional transition metal carbonitride Ti3CNTx for ultrafast supercapacitors, J. Mater. Chem. A 10 (2022) 18812–18821.
[22] Y. Zhang, Q. Jin, L. Li, M. Zhang, J. Wen, L. Wu, H. Gao, X. Zhang, L. Li, In-situ synergistic W18O49/Ti3C2Tx heterostructure as negative electrode for high energy density supercapacitors, Carbon 208 (2023) 92–101.
[23] Y. Liu, J. Yu, D. Guo, Z. Li, Y.J.J.o.A. Su, Compounds, Ti3C2Tx MXene/graphene nanocomposites: synthesis and application in electrochemical energy storage, J. Alloys Compoun. 815 (2020) 152403.
[24] Y.T. Liu, X.D. Zhu, L.J.S. Pan, Hybrid architectures based on 2D MXenes and lowdimensional inorganic nanostructures: methods, synergies, and energy-related applications, Small 14 (2018) 1803632.
[25] T. Li, L. Yao, Q. Liu, J. Gu, R. Luo, J. Li, X. Yan, W. Wang, P. Liu, B. Chen, W. Zhang, W. Abbas, R. Naz, D. Zhang, Fluorine-free synthesis of high-purity Ti3C2Tx (T=OH, O) via alkali treatment, Angew. Chem. Int. Ed. 57 (2018) 6115–6119.

[26] A.M. Aravind, M. Tomy, A. Kuttapan, A.M. Kakkassery Aippunny, X.T. Suryabai, Progress of 2D MXene as an electrode architecture for advanced supercapacitors: a comprehensive review, ACS Omega 8 (2023) 44375–44394.
[27] L. Wang, Y. Tan, Z. Yu, H. Tian, Y. Lai, Y. He, H. Xiang, J. Wang, W. Zhao, L. Zhang, Three-dimensional polyaniline architecture enabled by hydroxyl-terminated Ti3C2Tx MXene for high-performance supercapacitor electrodes, Mater. Chem. Front. 5 (2021) 7883–7891.
[28] Z. Bo, Z. Huang, Z. Zheng, Y. Chen, J. Yan, K. Cen, H. Yang, K. Ken Ostrikov, Accelerated ion transport and charging dynamics in more ionophobic sub-nanometer channels, Energy Storage Mater. 59 (2023) 102797.
[29] S. Gong, F. Zhao, H. Xu, M. Li, J. Qi, H. Wang, Z. Wang, X. Fan, C. Li, J. Liu, Iodine-functionalized titanium carbide MXene with ultra-stable pseudocapacitor performance, J. Colloid Interface Sci. 615 (2022) 643–649.
[30] R.B. Rakhi, B. Ahmed, M.N. Hedhili, D.H. Anjum, H.N. Alshareef, Effect of postetch annealing gas composition on the structural and electrochemical properties of Ti2CTx MXene electrodes for supercapacitor applications, Chem. Mater. 27 (2015) 5314–5323.
[31] M. Han, X. Yin, H. Wu, Z. Hou, C. Song, X. Li, L. Zhang, L. Cheng, Ti3C2 MXenes with modified surface for high-performance electromagnetic absorption and shielding in the X-band, ACS Appl. Mater. Interfaces 8 (2016) 21011–21019.
[32] V. Kamysbayev, A.S. Filatov, H. Hu, X. Rui, F. Lagunas, D. Wang, R.F. Klie, D. V. Talapin, Covalent surface modifications and superconductivity of two-dimensional metal carbide MXenes, Science 369 (2020) 979–983.
[33] W. Liu, Y. Zheng, Z. Zhang, Y. Zhang, Y. Wu, H. Gao, J. Su, Y. Gao, Ultrahigh gravimetric and volumetric capacitance in Ti3C2Tx MXene negative electrode enabled by surface modification and in-situ intercalation, J. Power Sources 521 (2022) 230965.
[34] V. Buravets, A. Olshtrem, V. Burtsev, O. Gorin, S. Chertopalov, A. Chumakov, M. Schwartzkopf, J. Lancok, V. Svorcik, O. Lyutakov, E. Miliutina, Plasmon assisted Ti3C2Tx grafting and surface termination tuning for enhancement of flake stability and humidity sensing performance, Nanoscale Adv. 5 (2023) 6837–6846.
[35] A. Olshtrem, I. Panov, S. Chertopalov, K. Zaruba, B. Vokata, P. Sajdl, J. Lancok, J. Storch, V. Církva, V. Svorcik, M. Kartau, A.S. Karimullah, J. Vana, O. Lyutakov, Chiral plasmonic response of 2D Ti3C2Tx flakes: realization and applications, Adv. Funct. Mater. 33 (2023) 2212786.
[36] A. Olshtrem, S. Chertopalov, O. Guselnikova, R.R. Valiev, M. Cieslar, E. Miliutina, R. Elashnikov, P. Fitl, P. Postnikov, J. Lancok, V. Svorcik, O. Lyutakov, Plasmon-assisted MXene grafting: tuning of surface termination and stability enhancement, 2D Mater. 8 (2021) 045037.
[37] A. Iqbal, J. Hong, T.Y. Ko, C.M. Koo, Improving oxidation stability of 2D MXenes: synthesis, storage media, and conditions, Nano Converg 8 (2021) 9.
[38] R.A. Soomro, P. Zhang, B. Fan, Y. Wei, B. Xu, Progression in the oxidation stability of MXenes, Nano-Micro Lett. 15 (2023) 108.
[39] A. Olshtrem, E. Miliutina, P. Sajdl, V. Burtsev, M. Erzina, M. Vondracek, P. Postnikov, J. Lancok, V. Svorcik, S. Chertopalov, O. Lyutakov, Plasmon-assisted spatially selective grafting of Ti3C2TX flakes for prevention of MXene oxidation and stability increase, Chem. Eng. J. 476 (2023) 146399.
[40] V. Neubertova, O. Guselnikova, Y. Yamauchi, A. Olshtrem, S. Rimpelova, E. Čižmár, M. Orendáč, J. Duchon, L. Volfova, J. Lancok, V. Herynek, P. Fitl, P. Ulbrich, L. Jelinek, P. Schneider, J. Kosek, P. Postnikov, Z. Kolska, V. Svorcik, S. Chertopalov, O. Lyutakov, Covalent functionalization of Ti3C2T MXene flakes with Gd-DTPA complex for stable and biocompatible MRI contrast agent, Chem. Eng. J. 446 (2022) 136939.
[41] Y. Zhou, K. Maleski, B. Anasori, J.O. Thostenson, Y. Pang, Y. Feng, K. Zeng, C. B. Parker, S. Zauscher, Y. Gogotsi, J.T. Glass, C. Cao, Ti3C2Tx MXene-reduced graphene oxide composite electrodes for stretchable supercapacitors, ACS Nano 14 (2020) 3576–3586.
[42] C. Li, S. Wang, X. Wang, W. Bai, H. Sun, F. Pan, Y. Chi, Z. Wang, High-temperature supercapacitors based on MXene with ultrahigh volumetric capacitance, ACS Mater. Lett. 5 (2023) 2084–2095.
[43] W. Zheng, J. Halim, J. Rosen, M.W. Barsoum, Aqueous electrolytes, MXene-based supercapacitors and their self-discharge, Adv. Energy Sustain. Res. 3 (2022) 2100147.
[44] E.A. Chernova, D.I. Petukhov, A.P. Chumakov, A.V. Kirianova, I.S. Sadilov, O. O. Kapitanova, O.V. Boytsova, R.G. Valeev, S.V. Roth, A.A. Eliseev, A.A. Eliseev, The role of oxidation level in mass-transport properties and dehumidification performance of graphene oxide membranes, Carbon 183 (2021) 404–414.
[45] Y. Li, C. Pan, P. Kamdem, X.-J. Jin, Binder-free two-dimensional MXene/acid activated carbon for high-performance supercapacitors and methylene blue adsorption, Energy Fuels 34 (2020) 10120–10130.
[46] X. Wei, M. Cai, F. Yuan, D. Lu, C. Li, H. Huang, S. Xu, X. Liang, W. Zhou, J. Guo, The surface functional modification of $Ti_3C_2T_x$ MXene by phosphorus doping and its application in quasi-solid state flexible supercapacitor, Appl. Surf. Sci. 606 (2022) 154817.
[47] R. Ma, X. Zhang, J. Zhuo, L. Cao, Y. Song, Y. Yin, X. Wang, G. Yang, F. Yi, Self-supporting, binder-free, and flexible $Ti_3C_2T_x$ MXene-based supercapacitor electrode with improved electrochemical performance, ACS Nano 16 (2022) 9713–9727.
[48] J. Chen, M. Chen, W. Zhou, X. Xu, B. Liu, W. Zhang, C. Wong, Simplified synthesis of fluoride-free $Ti_3C_2T_x$ via electrochemical etching toward high-performance electrochemical capacitors, ACS Nano 16 (2022) 2461–2470.
[49] H. Hwang, S. Byun, S. Yuk, S. Kim, S.H. Song, D. Lee, High-rate electrospun $Ti_3C_2T_x$ MXene/carbon nanofiber electrodes for flexible supercapacitors, Appl. Surf. Sci. 556 (2021) 149710.
[50] K. Donthula, R. Araga, N. Thota, S. Sundarrajan, S. Ramakrishna, M. Kakunuri, Hierarchically structured carbon nanofibers with embedded MXene and coated with cobalt oxide as a high-performance electrode for supercapacitors, J. Energy Storage 83 (2024) 110686.
[51] L. Luo, Y. Zhou, W. Yan, G. Du, M. Fan, W. Zhao, Construction of advanced zeolitic imidazolate framework derived cobalt sulfide/MXene composites as high-performance electrodes for supercapacitors, J. Colloid Interface Sci. 615 (2022) 282–292.
[52] W. Luo, Y. Wei, Z. Zhuang, Z. Lin, X. Li, C. Hou, T. Li, Y. Ma, Fabrication of $Ti_3C_2T_x$ MXene/polyaniline composite films with adjustable thickness for high-performance flexible all-solid-state symmetric supercapacitors, Electrochim. Acta 406 (2022) 139871.
[53] X. Zhang, H. Liu, X. Lu, R. Xu, Y. Niu, α-Fe_2O_3@C/MXene composites with core-shell structures applied as electrodes for pseudo-supercapacitors, J. Alloys Compd. 983 (2024) 173522.
[54] Z. Fan, Y. Wang, Z. Xie, D. Wang, Y. Yuan, H. Kang, B. Su, Z. Cheng, Y. Liu, Modified MXene/holey graphene films for advanced supercapacitor electrodes with superior energy storage, Adv. Sci. 5 (2018) 1800750.
[55] M. Mahmood, A. Rasheed, I. Ayman, T. Rasheed, S. Munir, S. Ajmal, P.O. Agboola, M.F. Warsi, M. Shahid, Synthesis of ultrathin MnO_2 nanowire-intercalated 2D-MXenes for high-performance hybrid supercapacitors, Energy Fuels 35 (2021) 3469–3478.
[56] H. Zhou, Y. Lu, F. Wu, L. Fang, H. Luo, Y. Zhang, M. Zhou, MnO_2 nanorods/MXene/CC composite electrode for flexible supercapacitors with enhanced electrochemical performance, J. Alloys Compd. 802 (2019) 259–268.
[57] Y. Wang, N. Chen, Y. Liu, X. Zhou, B. Pu, Y. Qing, M. Zhang, X. Jiang, J. Huang, Q. Tang, B. Zhou, W. Yang, MXene/Graphdiyne nanotube composite films for Free-Standing and flexible Solid-State supercapacitor, Chem. Eng. J. 450 (2022) 138398.
[58] W. Liu, Y. Zheng, Z. Zhang, Y. Zhang, Y. Wu, H. Gao, J. Su, Y. Gao, Ultrahigh gravimetric and volumetric capacitance in $Ti_3C_2T_x$ MXene negative electrode enabled by surface modification and in-situ intercalation, J. Power Sources 521 (2022) 230965.
[59] H. Li, S. Lin, H. Li, Z. Wu, L. Zhu, C. Li, X. Zhu, Y. Sun, Highly stable and uniformly dispersed 1T-MoS_2 nanosheets co-induced by chemical pressure and 2D template method with high supercapacitor performance, J. Mater. Chem. A 10 (2022) 7373–7381.
[60] M. Ghidiu, M.R. Lukatskaya, M.-Q. Zhao, Y. Gogotsi, M.W. Barsoum, Conductive two-dimensional titanium carbide 'clay' with high volumetric capacitance, Nature 516 (2014) 78–81.
[61] K. Li, X. Wang, S. Li, P. Urbankowski, J. Li, Y. Xu, Y. Gogotsi, An ultrafast conducting Polymer@MXene positive electrode with high volumetric capacitance for advanced asymmetric supercapacitors, Small 16 (2020) 1906851.
[62] M. Boota, B. Anasori, C. Voigt, M.-Q. Zhao, M.W. Barsoum, Y. Gogotsi, Pseudocapacitive electrodes produced by oxidant-free polymerization of pyrrole between the layers of 2D titanium carbide (MXene), Adv. Mater. 28 (2016) 1517–1522.
[63] A. Yadav, S. Singal, J. Kumar, R.K. Sharma, Sonochemically synthesized porous V_2CT_x MXene/red-black phosphorus composite: a promising electrode for supercapacitors, J. Energy Storage 79 (2024) 110155.
[64] C. Li, G. Jiang, M. Demir, Y. Sun, R. Wang, T. Liu, Preparation of rGO/MXene@NiCo-P and rGO/MXene@Fe_2O_3 positive and negative composite electrodes for high-performance asymmetric supercapacitors, J. Energy Storage 56 (2022) 105986.
[65] C. Peng, Z. Kuai, T. Zeng, Y. Yu, Z. Li, J. Zuo, S. Chen, S. Pan, L. Li, WO_3 Nanorods/MXene composite as high performance electrode for supercapacitors, J. Alloys Compd. 810 (2019) 151928.
[66] M.R. Lukatskaya, O. Mashtalir, C.E. Ren, Y. Dall'Agnese, P. Rozier, P.L. Taberna, M. Naguib, P. Simon, M.W. Barsoum, Y. Gogotsi, Cation intercalation and high volumetric capacitance of two-dimensional titanium carbide, Science 341 (2013) 1502–1505.